Available online at www.sciencedirect.com

SciVerse ScienceDirect

Ceramics International 39 (2013) 7861–7867

CERAMICS INTERNATIONAL

www.elsevier.com/locate/ceramint

# Multivariate optimization of the synthesis of titania biomorphic ceramics and development of a FT-IR method for quantification synthesis yield

M.M. López Guerrero, E. Vereda Alonso*, A. Garcíade Torres, M. López Claros, J.M. Cano Pavón

*Department of Analytical Chemistry, Faculty of Sciences, University of Malaga, 29071 Malaga, Spain*

Received 9 January 2013; received in revised form 14 March 2013; accepted 14 March 2013
Available online 25 March 2013

**Abstract**

Titania biomorphic ceramics were manufactured from wood preforms by a two steps process, i.e. infiltration and then pyrolysis in an inert atmosphere to produce porous TiC ceramics, followed by infiltration and pyrolysis in an air atmosphere where TiC was oxidized to $TiO_2$. This technology provides a cost effective and eco-friendly route to advanced ceramic materials. The properties of biomorphic ceramics depend decisively on the synthesis parameters, that were optimized using a multivariate methodology for the design of experiments. Four variables (infiltration time, titanium isopropoxide and acetic acid proportion, and number of infiltrations before and after pyrolysis) were considered as factors in the synthesis optimization process. Interactions between these factors and their optimal levels were investigated using a two level factorial design. For evaluating the yields, a new method by Fourier transform infrared spectrometry (FTIR) has been developed for the direct determination of $TiO_2$ by absorbance measurements in KBr pellets. The procedure is based on the use of the ratio between the absorbance of the characteristic band of titania and those of a nitrate internal standard added to samples. A multivariate calibration strategy based on inverse least squares approach was employed for quantification.


*Keywords:* Fourier transform infrared spectroscopy; Multivariate calibration; Ceramic materials; Titania oxide; Multivariate optimization

## 1. Introduction

Materials synthesized from biological structures have become of increasing interest in the last decade. Various biotemplating high temperature techniques have been developed to use natural grown structure, e.g. wood, natural fibers or paper, as template for conversion into technical ceramics and ceramic composites. The wood structure is characterized by cells and vessels that are filled with water, with 3–0 and 3–1 connectivities, respectively. The size of the cells and the diameter of the vessels both vary from species to species. Wood is recognized as one of the best and most intricate engineering materials created by nature and known to mankind [1,2]. These features in wood make it an attractive template for making special porous ceramics such as filters, absorbents and catalyst supports, machinable ceramics, and light structural ceramics. Biostructure derived from titanium oxide is of particular importance for its application as heat insulation, filter, catalyst support in high temperature processes and for medical implants [3], bioactive ceramic $TiO_2$ is one of the most promising biocompatible materials [4,5]. Photocatalysis currently receives enormous attention because of its potential application in environmental treatment and fine chemical synthesis [6–14].

Different biotemplating technologies for conversion of bioorganic preformed materials into structural ceramics and ceramic composites have been developed in recent years [15–17]. The reactive techniques involve conversion of the bioorganic preforms in biocarbon templates by pyrolysis in inert atmosphere. Then, they are infiltrated with precursor systems to produce porous TiC ceramics, which are oxidized in air at temperatures of 1250 °C. In general, two different approaches have been applied to convert the biological preforms into non-oxide as well as oxide substitution ceramics. Conventionally, titania is prepared from inorganic precursors, mainly by thermal hydrolysis of titanium (IV) compounds in highly acidic solutions, or by thermal oxidation of $TiCl_4$ vapor at high temperature regimes [18]. Ota et al. produced biomorphous oxide ceramics by infiltration of wood materials with metal alkoxide, e.g. titanium isopropoxide [19]. After high temperature treatment in air, the wood structures were

*Corresponding author. Tel.: +34 9521 31883; fax: +34 952 132 000.
*E-mail addresses:* eivereda@gmail.com, eivereda@uma.es (E. Vereda Alonso).

0272-8842/$ - see front matter © 2013 Elsevier Ltd and Techna Group S.r.l. All rights reserved.
http://dx.doi.org/10.1016/j.ceramint.2013.03.047

converted into porous $TiO_2$-ceramics. In the sol–gel method [20] a variety of titanium (IV) alkoxides are dispersed in non-reactive organic solvents and then hydrolyzed. For a good reproduction of natural biomorph structures, a liquid precursor is favorable, and the sol–gel method is very suitable, considering its advantages like chemical flexibility, facile shape control, and mild reaction conditions. The chemistry involved is rather complex. Reactions such as hydrolysis, esterification, alcoholic condensation, water condensation, and alcoholysis occur successively and consecutively, and lead eventually to a dispersed gel or a precipitate [21].

FTIR is potentially a good tool for structural studies of these types of materials, however, this technique has only been used by a few authors [22–25] to investigate the carbothermal conversion of the charcoal silica composites into SiC in the final step of the synthesis. Although FTIR is a rapid analytical technique that provides information about the qualitative composition of samples, quantitative analysis requires the use of cells of known thickness and in general, a previous dilution of the samples with a suitable solvent. These limitations often preclude the general application of this technique to quantitative determinations. In recent years, a series of simple models for carrying out quantitative determinations from infrared data, which do not require the use of a known absorption pathlength, have been described [22–29]. These models are based on the use of the ratio of the absorbance at two well-defined wavenumbers; however, the use of the ratio of the characteristic bands of two compounds in a mixture does not permit the determination of the concentration of each component, and only the proportion of two compounds considered was obtained. This problem can be solved if the concentration of one of the compounds is known; thus it is possible when this compound is an adequate internal standard [30].

The aim of this paper has been the optimization of the experimental conditions for the synthesis of titania biomorphic ceramics and the development of simple strategies which could be used for routine determination of $TiO_2$ in these ceramics based on the use of FTIR absorbance measurements in KBr pellets. The simplest procedure was based on the use of the ratio between the absorbance of the characteristic band of $TiO_2$ at 557 $cm^{-1}$ and three intense bands at 2714, 2416 and 1388 $cm^{-1}$ of an internal standard (sodium nitrate) added to samples. A multivariate calibration strategy based on inverse least squares approach was employed for quantification. Three different woods of varying density and pore size were chosen as precursors (beech, mongoy and cherry). The results that are obtained for all ceramics studied were satisfactorily compared with those obtained by X-ray diffractometry (XRD). The proposed method was also applied to the analysis of synthetic samples prepared by mixing pyrolyzed wood with pure $TiO_2$, and the results indicated good recovery in all instances.

## 2. Experimental

### 2.1. Reagents

Analytical reagent grade chemicals were used throughout. Potassium bromide, and sodium nitrate were purchased from Merck (Darmstadt, Germany) and titanium oxide (99.9% w/w) from Alfa Aesar (Royston, England). Titania sol was obtained from titanium (IV) isopropoxide ($Ti(OPr)_4$) 99.9% pure liquid from Aldrich (Steinheim, Germany). Solvents, methanol and acetic acid glacial were all from Merck (Darmstadt, Germany). All these reagents were dried at 48 °C for 24 h and conserved into a desiccator.

### 2.2. Synthesis of titania biomorphic ceramics

Sol–gel process involves hydrolysis of the sol and drying to form a gel. Sol–gel process can be applied to most of the templates; in this case different kinds of biomorphic ceramics derived from natural woods (beech, cherry and mongoy) were prepared for the sol–gel infiltration process. For the preparation of the $TiO_2$–sol, titanium isopropoxide was modified with acetic acid (isoproxide/acetic acid ratio: 7) and subsequent hydrolysis in distilled $H_2O$. More details of the sol procedure can be found in elsewhere [7,31]. This method has been widely employed to synthesize a variety of biomorphic materials.

Rectangular specimens (3 cm × 1 cm × 1 cm) of the carbon preform were cut perpendicular to the native wood axis. The samples were dried at 70 °C for 24 h, and subsequently vacuum infiltrated (60 min) with the $TiO_2$ sol. The infiltrated samples were dried in air at 130 °C for 2 h to form the gel in the wood cells after infiltration. This procedure was repeated up to seven times to achieve a higher content of $TiO_2$ precursor in the wood. Afterward, the samples were pyrolyzed at 800 °C for 1 h in Ar-atmosphere. At this temperature the biopolymers (cellulose, hemicellulose and lignin) of wood were decomposed, leaving a porous carbon char. During pyrolysis, a low heating rate (1.5 °C $min^{-1}$) was adopted to avoid damage in the wood cell walls by gas release. The infiltration and drying process were repeated up to three times to increase the $TiO_2$ content in the biomorphic samples. Finally the specimens were held at 1250 °C for 1 h in air-atmosphere to allow the complete reaction of titania to form $TiO_2$, in order to remove the carbon template by oxidation and to increase the density of the $TiO_2$ by sintering.

The hydrolysis reaction of ($Ti(OPr)_4^i$) may be expressed as

$$(Ti(OPr)_4^i) + xH_2O \rightarrow TiO_2 + yH_2O + 4PrOH$$

The processing scheme is summarized in Fig. 1.

### 2.3. Instrumentation

The infrared spectroscopy measurements were carried out using a Perkin-Elmer Fourier transform infrared spectrometer, Spectrum 100 (Perkin-Elmer, Concord, Canada). The spectra were recorded in the range 4000–450 $cm^{-1}$ with a resolution of 4 $cm^{-1}$. Potassium bromide pellets were used to obtain the IR spectra of the samples. Pellets with 13 mm diameter were pressed at 7 ton for 10 min in an evacuated pellet die from 150 mg mixture of sample, sodium nitrate and potassium bromide. For mass measurements an AND GR-202 balance was used with a precision of ± 0.01 mg. Multivariate calibration and optimization were carried out using Statgraphics Centurion software (version 16.1.11 for windows).

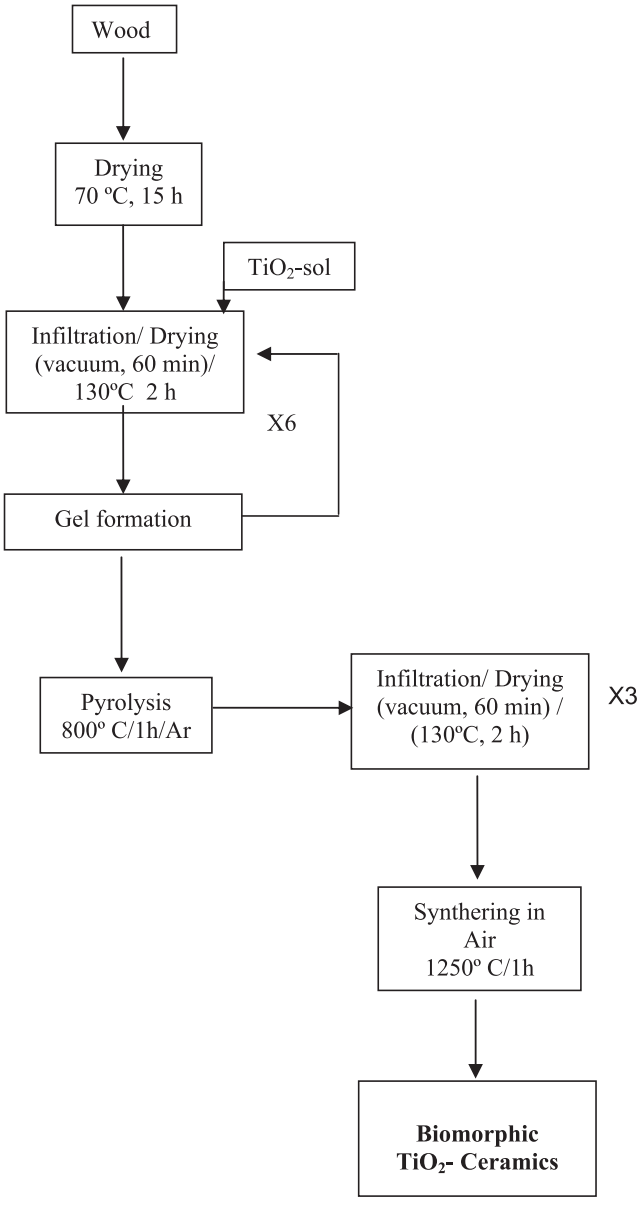


Fig. 1. Processing scheme of manufacturing $TiO_2$ ceramics from wood.

For validation purposes of the IR-measurents, X-ray diffractometry (XRD, D 500, Siemens, Kar-Isruhe, Germany) was used. As an example, XRD pattern of a biomorphic ceramic is shown in Fig. 2. Distinct peaks of the rutile $TiO_2$ can be observed at $2\theta = 27.4^o$, $36.1^o$, $41.3^o$, $54.3^o$, $56.6^o$ and $69.0^o$; in addition to these lines the peak at $2\theta = 25.2^o$ can be attributed to carbon. The degree of conversion of the biocarbon char template into $TiO_2$ depends on the type of wood. Other weak peaks were attributed to impurities present in the samples.

A Lenton Tube Furnace, model LTF 16/180, was employed for the synthesis of biomorphic ceramics.

### 2.4. Preparation of calibration set for $TiO_2$ determination

Standard KBr pellets were prepared by mixing different accurately weighed amounts from 0.0 mg to 16.0 mg ($\pm$ 0.01 mg) of $TiO_2$, 2.0 mg internal standard (sodium nitrate), and KBr to complete a total amount of 150.0 mg ($\pm$ 0.01 mg). Sample pellets were prepared by mixing 10.0 mg of biomorphic ceramic (previously ground and homogenized), 2.0 mg internal standard and KBr to complete a total amount of 150.0 mg. The mixtures were homogenized for 5 min in an agate mortar. For the background spectrum, a pellet was prepared with 150.0 mg ($\pm$ 0.01 mg) of KBr.

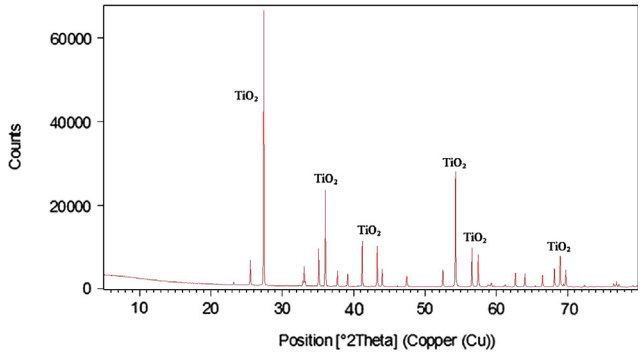


Fig. 2. XRD spectrum of biomorphic ceramic from mongoy.

Table 1
Baseline established for integrating areas in FTIR analysis.

| $\nu$ ($cm^{-1}$) | $X_{min}$ ($cm^{-1}$) | $X_{max}$ ($cm^{-1}$) |
|---|---|---|
| 2714 | 2730 | 2890 |
| 2416 | 2409 | 2538 |
| 1388 | 1360 | 1403 |
| 557 | 450 | 813 |

The spectra were recorded from 4000 to 450 $cm^{-1}$, using a nominal resolution of 4 $cm^{-1}$ and accumulating 50 scans per spectrum. Once registered, peak areas were measured for the band corresponding to $TiO_2$ (557 $cm^{-1}$) and the ones corresponding to the internal standard, nitrate (2714, 2416 and 1388 $cm^{-1}$), using the baselines given in Table 1 for each peak. The $TiO_2$ concentration was determined by a multivariate calibration strategy of inverse least squares, where several instrumental responses ($r_1$,$r_2$,$r_3$,…$r_n$) were used:

$$[TiO_2]_{sample} = b_0 + b_1 r_1 + b_2 r_2 + b_3 r_3 + \ldots b_n r_n \quad (1)$$

The responses ($r_1$,$r_2$,$r_3$,…$r_n$) are the quotients between the peak area corresponding to $TiO_2$ (557 $cm^{-1}$) and the peak areas corresponding to the nitrate bands (2714, 2416 and 1388 $cm^{-1}$); and $b_0$, $b_1$, $b_2$, $b_3$ and $b_n$ are the regression coefficients. Therefore, an equation with four unknowns is obtained ($b_0$, $b_1$, $b_2$, and $b_3$). If $I$ standards are prepared and measured there will be a system of $I$ equations with four unknowns. Obviously, at least four standards must be made. Once the regression equation is known, the $TiO_2$ concentration in the sample is calculated (Eq. 1).

### 2.5. Optimization strategy of the synthesis

A factorial design $2^4$ (16 experiments) was developed to optimize the synthesis of the titania biomorphic ceramics.

The selected factors and their corresponding ranges were determined after preliminary experiments. These factors were the infiltration time, the titanium isopropoxide and acetic acid proportion, and the number of infiltrations before and after pyrolysis. The lower and upper values given to each factor are shown in Table 2.

## 3. Results and discussion

### 3.1. FTIR determination of $TiO_2$

#### 3.1.1. Selection of the appropriate bands for the FTIR measurement of $TiO_2$

Fig. 3 shows the FTIR spectra of KBr pellets of pure $TiO_2$ and sodium nitrate. As can be seen in the case of pure $TiO_2$, a broad band at 557 $cm^{-1}$ was found which was assigned to the envelope of the phonon bands of Ti–O–Ti [32]. For sodium nitrate three bands were located at 2714, 2416 and 1388 $cm^{-1}$. The band at 1388 $cm^{-1}$ was assigned to the asymmetric stretching vibration and bands at 2714 and 2416 were assigned to symmetric plus asymmetric stretching vibrations [33]. As can be seen in Fig. 3 there were no overlaps between the $TiO_2$ band and nitrate bands, so these bands were appropriate to be employed for $TiO_2$ determination.

Table 2
Factor levels in the screening design ($2^4$).

| Variable | Lower | Upper |
|---|---|---|
| Titanium isopropoxide/acetic acid proportion | 4 | 7 |
| Infiltration time (min) | 15 | 60 |
| Number of infiltrations before pyrolysis | 3 | 6 |
| Number of infiltrations after pyrolysis | 3 | 6 |

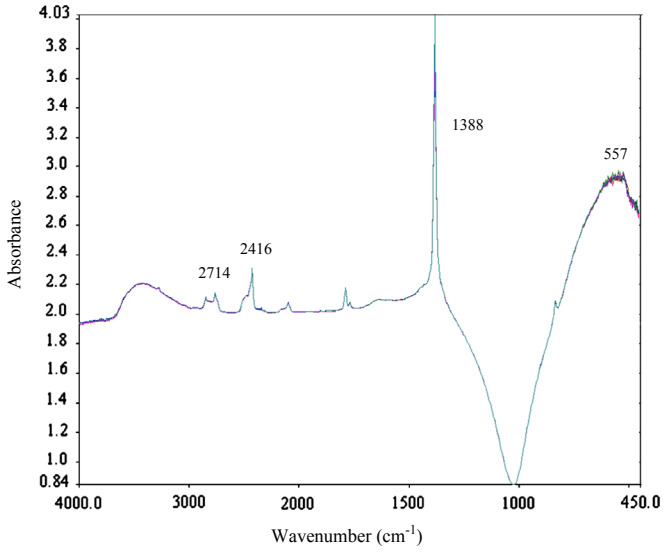


Fig. 3. FTIR spectrum of a KBr disk of $TiO_2$ biomorphic ceramic from mongoy with sodium nitrate as the internal standard.

#### 3.1.2. Selection of the instrumental parameters and conditions of measurement

Absorbance measurements in the solid phase are usually affected by larger levels of noise than those found in homogeneous solutions due to the presence of the solid support, which causes a strong attenuation of the light intensity reaching the detector. Thus, a careful study of the instrumental parameters and conditions of measurement was carried out in order to obtain the best signal-to-noise ratio possible, which would ensure satisfactory reproducible data.

The $TiO_2$ band at 557 $cm^{-1}$ and sodium nitrate bands at 2714, 2416 and 1388 $cm^{-1}$ were used in this study. Band heights were measured at these wavenumbers and areas were calculated by drawing the baselines shown in Table 1. The height and area ratios were studied, obtaining the best results with the area ratios.

A systematic study of the effect of the nominal resolution and the number of accumulated scans was performed under the aforementioned conditions. The number of accumulated scans per spectrum was studied from 20 to 250; the nominal resolution varied from 0.05 to 32 $cm^{-1}$. An increase in the number of accumulated scans had no influence on the height or area ratios but it reduces the background drastically. So, 50 scans were established as suitable for FTIR measurements in order to ensure a compromise between measurements frequency and precision of the values. On the other hand, the most intense signals were found for a 4 $cm^{-1}$ nominal resolution, this value also corresponding to the best repeatability.

The amount of sample to prepare the KBr disk and the total weight of the pellet were also optimized; the amount of biomorphic ceramic was varied from 0.5 to 20 mg maintaining the total weight of the mix as 150 mg. The most intense signal at the bands of interest was that with 10 mg of sample (6.67% in biomorphic ceramic), with this concentration in biomorphic ceramic the total weight of the pellet was varied from 60 to 200 mg; a decrease in disk weight produces more transparent disks, but more fragile, and so 150 mg was established for suitable FTIR measurements in order to ensure resistant KBr disks.

#### 3.1.3. Quantitative analysis of FTIR data

Simple linear regression (SLR) and multiple linear regression (MLR) were proved with each of the three area ratios chosen between the analyte and the internal standard, obtaining the best results with the MLR method. As an example, the observed versus predicted graph and the equation of the fitted model for $TiO_2$ determination in the biomorphic ceramic are given in Fig. 4.

To test the applicability of the method, synthetic samples were prepared by mixing pyrolyzed wood with pure $TiO_2$ and were analyzed by using the proposed method. The results shown in Table 3 indicated good recoveries in all instances. For validation purposes three biomorphic ceramics from cherry, beech and mongoy were analyzed by the proposed IR method and XRD. The results obtained for all biomorphic ceramics studied (Table 4) were satisfactorily compared with

$$[TiO_2] = -0.0451 + 0.24\frac{A_{557}}{A_{2714}} - 0.53\frac{A_{557}}{A_{2416}} + 0.29\frac{A_{557}}{A_{1288}}$$

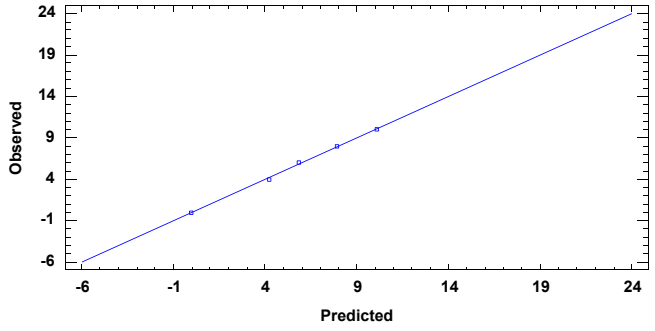


Fig. 4. The observed versus predicted graphs and the equation of the fitted model for the biomorphic ceramic for $TiO_2$ determination.

Table 3
Results of the determination of $TiO_2$ for synthetic samples.

| Content of the synthetic samples (% $TiO_2$) | FTIR analysis (% $TiO_2$) | Recovery (%) |
|---|---|---|
| 40 | $38.6 \pm 1.6$ | 96.5 |
| 50 | $50.2 \pm 1.1$ | 100.4 |
| 60 | $60.4 \pm 3.4$ | 100.7 |

Table 4
Results of the determination of $TiO_2$ in biomorphic ceramic by XRD and FTIR.

| Biomorphic ceramics from | XRD (% $TiO_2$) | FTIR (% $TiO_2$) |
|---|---|---|
| Cherry wood | $51.5 \pm 0.3$ | $50.8 \pm 3.6$ |
| Beech | $63.8 \pm 0.3$ | $61.3 \pm 2.4$ |
| Mongoy | $73.5 \pm 0.3$ | $73.4 \pm 2.7$ |

those obtained by XRD analysis, according to the *t*-test for a confidence level of 5% indicating that the multivariate calibration approach using KBr pellets with nitrate as internal standard and MLR is useful for the determination of $TiO_2$ in biomorphic materials.

### 3.2. Optimization of the synthesis of $TiO_2$ biomorphic ceramic

#### 3.2.1. Selection of the precursor materials

Wood can be classified as either softwood or hardwood. Softwoods have one type of pore in the plane perpendicular to the growth direction (axial plane) while hardwoods tend to have two types of pores in this plane. In hardwoods, the smaller pores with thicker cell walls are referred to as fiber cells which provide strength to the tree. The larger pores with thinner cell walls are referred to as sap channels which allow the conduction of fluids throughout the tree. The hardwoods with uniformly distributed small sap channels can be referred to as uniformly distributed pore (UDP) hardwoods, e.g. beech, and the hardwoods with relatively large sap channels are not uniformly distributed pore (NUDP) hardwoods, e.g. oak [19]. UDP hardwoods have been shown to be adequate templates to synthesize biomorphic ceramics [34]. Thus, in this work three hardwoods were tested as templates: cherry, beech and mongoy. From the analysis of the biomorphic ceramics synthesized with these hardwoods (Table 4) it can be seen that mongoy shows the best yields in $TiO_2$. So, mongoy wood was chosen as precursor to optimize the synthesis of biomorphic ceramics.

#### 3.2.2. Factorial design

Two level factorial designs have many advantages, for example they are more efficient than studying one factor at a time. A factorial design allows the effect of several factors and even interactions between them to be determined with the same number of trials as are necessary to determine any one of the effects by itself with the same degree of accuracy.

Table 5
Variables and their levels in the synthesis optimization.

| Experiment number | Titanium isopropoxide/acetic acid proportion | Infiltration time (min) | Number of infiltrations before pyrolysis | Number of infiltrations after pyrolysis | $TiO_2$ (%) | RSD (%) |
|---|---|---|---|---|---|---|
| 1 | 4 | 30 | 4 | 5 | 55.7 | 5.1 |
| 2 | 7 | 15 | 6 | 6 | 52.0 | 1.6 |
| 3 | 6 | 60 | 4 | 6 | 66.1 | 6.1 |
| 4 | 7 | 45 | 4 | 3 | 105.5 | 4.0 |
| 5 | 6 | 45 | 3 | 4 | 61.3 | 3.3 |
| 6 | 7 | 60 | 3 | 5 | 73.2 | 4.3 |
| 7 | 5 | 60 | 5 | 3 | 71.6 | 3.5 |
| 8 | 6 | 30 | 6 | 3 | 50.4 | 6.8 |
| 9 | 4 | 45 | 5 | 6 | 74.9 | 7.6 |
| 10 | 6 | 15 | 5 | 5 | 77.3 | 3.1 |
| 11 | 5 | 30 | 3 | 6 | 53.1 | 4.2 |
| 12 | 5 | 45 | 6 | 5 | 81.1 | 8.9 |
| 13 | 5 | 15 | 4 | 4 | 57.4 | 1.5 |
| 14 | 4 | 15 | 3 | 3 | 55.5 | 0.8 |
| 15 | 7 | 30 | 5 | 4 | 103.4 | 2.3 |
| 16 | 4 | 60 | 6 | 4 | 82.4 | 7.5 |

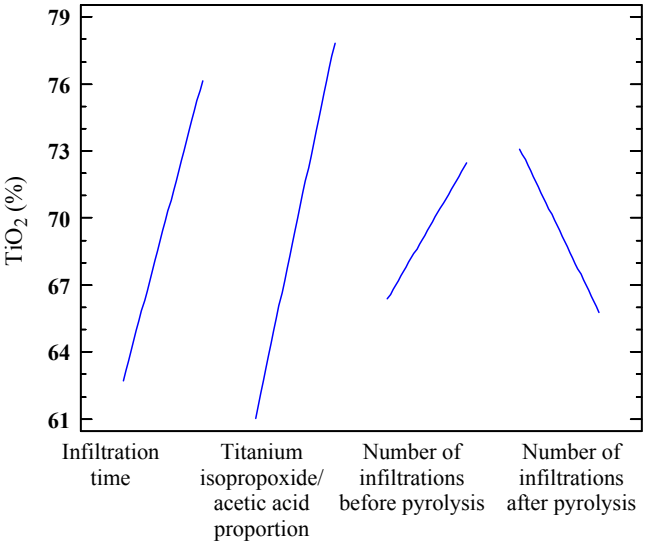


Fig. 5. Graph showing the influence of main effects on the synthesis of $TiO_2$.

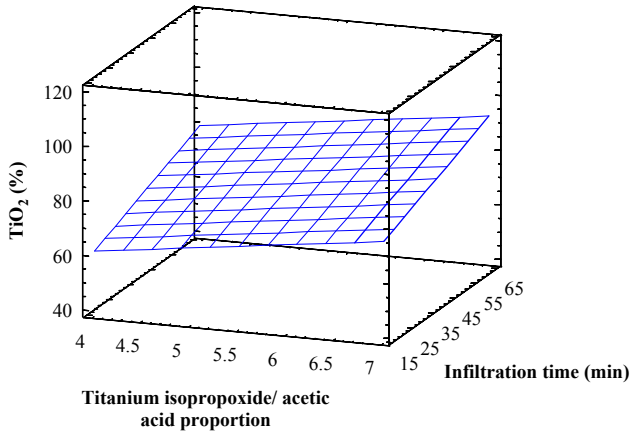


Fig. 6. Response surface estimated for the $2^4$ factorial design obtained by plotting the two main statistically significant factors.

A two level factorial design, $2^4$, involving 16 runs, was used to optimize the synthesis of the biomorphic $TiO_2$ ceramics. The selected response was the percentage of $TiO_2$ obtained in the synthesized ceramic. The variables to be optimized and the lower and upper values given to each factor are shown in Table 2. The experiments were randomly performed and the obtained data were processed by using the Statgraphics Centurion software. The experimental design matrix developed and the results obtained as % $TiO_2$ in the synthesized ceramic in each experiment are shown in Table 5.

In the main effects graph, shown in Fig. 5, it is observed that the infiltration time was the most significant factor (factor with the highest slope) followed by the titanium isopropoxide/acetic acid proportion, with a positive effect on the $TiO_2$ yield. On the other hand, the number of infiltrations before pyrolysis also has a positive influence on the synthesis yield, while the number of infiltrations after pyrolisis has a negative influence.

Fig. 6 shows the estimated response surface obtained for the experimental model developed using the significant factors: infiltration time and isopropoxide/acetic acid proportion. The optima conditions for the synthesis were the maxima values studied for three factors: titanium isopropoxide/acetic acid proportion: 7, infiltration time: 60 min, number of infiltrations before pyrolysis: 6; and the minimum value studied for the remaining factor, number of infiltrations after pyrolysis: 3.

Table 6
Results of the verification experiments of the synthesis.

| Synthesis | $TiO_2$ biomorphic ceramic (%) | RSD (%) |
|---|---|---|
| A | 100.6 | 7.7 |
| B | 81.9 | 3.5 |
| C | 84.5 | 5.1 |

A: titanium isopropoxide/acetic acid proportion—7, infiltration time—60 min, number of infiltrations before pyrolysis—6, and number of infiltrations after pyrolysis—3.
B: titanium isopropoxide/acetic acid proportion—7, infiltration time—60 min, number of infiltrations before pyrolysis—6, and number of infiltrations after pyrolysis—0.
C: titanium isopropoxide/acetic acid proportion—7, infiltration time—60 min, number of infiltrations before pyrolysis—3, and number of infiltrations after pyrolysis—3.

In order to verify the conclusions obtained from experimental design, three new experiments were performed by changing the number of infiltrations before and after pyrolysis. The results that are obtained are shown in Table 6. The $TiO_2$ yield obtained for experiment A was 100%. This experiment was performed with the optima conditions obtained by the factorial design.

## 4. Conclusions

The infiltration of wood (biological performs) with $TiO_2$ sol and heat treatment in the presence of air offers a simple process to manufacture $TiO_2$ biomorphic ceramics. The results obtained for $TiO_2$ in biomorphic ceramics show that FTIR, using the ratio of absorbance peak areas between the analyte and a reference compound, provides accurate results for the determination of $TiO_2$ in the samples with no need to use sample cells with a known optical pathlength. This method was used satisfactorily to optimize the synthesis process of these new materials. Using the optimized parameters, a synthesis yield near 100% was achieved.

## Acknowledgment

The authors thank the Spanish Ministerio de Ciencia y Tecnología (MCyT Project no. CTQ2099-07858) for supporting this study, and also FEDER funds.

## References

[1] Wood Handbook—Wood as an Engineering Material. Forest Products Laboratory, USDA Forest Service, Madison, WI. General Technical Report, FPL-GTR-113, 1999.
[2] A.P. Scniewind (Ed.), Pergamon Press, NY, 1989.
[3] C. Jing, Biotemplating of Highly Porous Oxide Ceramics, Ph.D. Thesis, Universität Erlangen-Nürnberg, Germany, 2005.
[4] E. Wintermantel, L. Cima, B. Shloo, R. Langer, Angiopolarity of cell carriers, directional angiogenesis in resorbable liver cell transplantation devices, in: R. Steiner, B. Weisz, R. Langer (Eds.), Angiogenesis:

Principles Science Technology Medicine, Birkhaeuser Verlag Basel Basel, Switzerland, 1992.
[5] H. Haugen, J. Will, A. Köhler, U. Hopfner, J. Aigner, E. Wintermantel, Ceramic $TiO_2$-foams: characterization of a potential scaffold, Journal of the European Ceramic Society 24 (2004) 661–668.
[6] A.L. Linsebigler, L. Guanquan, J.T.J. Yates, Photocatalysis on $TiO_2$ surfaces: principles, mechanisms, and selected results, Chemical Reviews 95 (3) (1995) 735–758.
[7] E.J. Wolfrum, J. Huang, D.M. Lake, P.C. Maness, Z. Huang, J. Fiest, W.A. Jacoby, Photocatalytic oxidation of bacteria, bacterial and fungal spores, and model biofilm components to carbon dioxide on titanium dioxide-coated surfaces, Environmental Science and Technology 36 (2002) 3412–3419.
[8] P. Greil, Biomorphous ceramics from lignocellulosics, Journal of the European Ceramic Society 21 (2001) 105–118.
[9] M. Miyaichi, A. Nakajima, A. Fujishima, K. Hashimoto, T. Watanabe, Photoinduced surface reactions on $TiO_2$ and $SrTiO_3$ films: photocatalytic oxidation and photoinduced hydrophilicity, Chemistry of Materials 12 (1) (2000) 3–5.
[10] Z. Zou, J. Ye, H. Arakawa, Surface characterization of nanoparticles of $NiO_x/In_{0.9}Ni_{0.1}TaO_4$: effects on photocatalytic activity, Journal of Physical Chemistry B 106 (2002) 13098–13101.
[11] C.J.G. Cornu, A.J. Colussi, M.R. Hoffmann, Quantum yields of the photocatalytic oxidation of formate in aqueous $TiO_2$ suspensions under continuous and periodic illumination, Journal of Physical Chemistry B 105 (2000) 1351–1354.
[12] R.R. Ozer, J.L. Ferry, Kinetic probes of the mechanism of polyoxometalate-mediated photocatalytic oxidation of chlorinated organics, Journal of Physical Chemistry B 104 (2000) 9444–9448.
[13] A. Maldotti, L. Andreotti, A. Molinari, S. Borisov, V. Vasilèv, Photoinitiated catalysis in Nafion membranes containing palladium (II) meso-tetrakis (N-methyl-4-pyridyl) porphyrin and iron (III) meso-tetrakis (2,6-dichlorophenyl) porphyrin for $O_2$-mediated oxidations of alkenes, Chemistry—A European Journal 7 (2001) 3564–3571.
[14] H. Einaga, S. Futamura, T. Ibusuki, Heterogeneous photocatalytic oxidation of benzene, toluene, cyclohexene and cyclohexane in humidified air: comparison of decomposition behavior on photoirradiated $TiO_2$ catalyst, Applied Catalysis B: Environmental 38 (2002) 215–225.
[15] C.R. Chenthamarakshan, Y. Ming, K.U. Rajeshwas, Underpotential photocatalytic deposition: a new preparative route to composite semiconductors, Chemistry of Materials 12 (2000) 3538–3540.
[16] H. Sieber, in: M. Singh et al.(Ed.), High Temperature Ceramic Matrix Composites-HTCMC-5, The American Ceramic Society Hoboken, NJ, USA, 2004, p. 407.
[17] H. Sieber, C. Hoffmann., A. Kaind, P. Greil, Biomorphic cellular ceramics, Advanced Engineering Materials 2 (3) (2000) 105–109.
[18] M. Visca, E. Matijevis, Preparation of uniform colloidal dispersions by chemical reactions in aerosols.I. Spherical particles of titanium dioxide, Journal of Colloid and Interface Science 68 (2) (1979) 304–319.
[19] T. Ota, M. Imaeda, H. Takase, M. Kobayashi, N. Kinoshita, T. Hirashita, H. Miyazaki, Y. Hikichi, Porous titania ceramic prepared by mimicking silicified wood, Journal of the American Ceramic Society 83 (6) (2000) 1521–1523.
[20] D. Segal, Chemical Synthesis of Advanced Ceramic Materials, Cambridge University Press, Cambridge, 1989.
[21] H. Schmidt, Chemistry of material preparation by the sol–gel process, Journal of Non-Crystalline Solids 100 (1988) 51–64.
[22] E. Vereda Alonso, A. García de Torres, M.T. Siles Cordero, J.M. Cano Pavón, Quantitative determinations of SiC and $SiO_2$ in new ceramic materials by Fourier transform infrared spectroscopy, Talanta 75 (2008) 424–431.
[23] M.M. López Guerrero, A. García de Torres, E. Vereda Alonso, M.T. Siles Cordero, J.M. Cano Pavón, Quantitative determination of ZrC in new ceramic materials by Fourier transform infrared spectroscopy, Ceramics Inernational 37 (2011) 607–613.
[24] J. Qian, J. Wang, Z. Jin, Preparation of biomorphic SiC ceramic by carbothermal reduction of oak wood charcoal, Materials Science and Engineering A 371 (2004) 229–235.
[25] J. Qian, J. Wang, G. Quiao, A. Jin, Preparation of porous SiC ceramic with a woodlike microstructure by sol–gel and carbothermal reduction processing, Journal of the European Ceramic Society 24 (2004) 3251–3259.
[26] M. de la Guardia Cirugeda, J.L. Carrión Dominguez, J. Medina Escriche, Use of infrared spectroscopy for the analysis of the average properties of nonylphenol-ethylene oxide condensates, Analyst 109 (4) (1984) 457–459.
[27] J.L. Carrión Domínguez, S. Sagrado, M. de la Guardia Cirugeda, Characterization of ethylene oxide/tertoctylphenol condensates by ultraviolet and infrared spectrometry, Analytica Chimica Acta 185 (1986) 101–107.
[28] Z.A. Benzo, C. Gómez, S. Menéndez, M. De la Guardia Cirugeda, A. Salvador, Some observations on the determination of the methyl parathion–parathion ratio in binary mixtures by infrared spectroscopy, Microchemical Journal 40 (1989) 271–276.
[29] S. Garrigues, M. de la Guardia Cirugeda, Mathematical models for the Fourier transform infrared spectroscopic determination of ortho-, meta-, para- xylene in xylol, Analyst 116 (1) (1991) 1159–1166.
[30] S. Garrigues, M. de la Guardia Cirugeda, Direct vapor generation Fourier transform infrared spectrometric determination of ethanol in blood, Analytica Chimica Acta 242 (1991) 123–129.
[31] Y. Shin, J. Liu, J.H. Chang, Z. Nie, G.J. Exarhos, Hierarchically ordered ceramics through surfactant-templated sol–gel mineralization of biological cellular structures, Advanced Materials 13 (10) (2001) 728–732.
[32] M.J. Velasco, R. Rubio, J. Rubio, J.L. Oteo, DSC and FT-IR analysis of the drying process of titanium alkoxide derived precipitates, Thermochimica Acta 326 (1999) 91–97.
[33] F. El-Kabbany, S. Taha, Temperature dependence of IR analysis of Sr $(NO_3)_2$, Thermochimica Acta 136 (1988) 7–18.
[34] E. Vereda Alonso, A. García de Torres, M.T. Siles Cordero, J.M. Cano Pavón, Multivariate optimization of the synthesis and of the microwave dissolution of biomorphic silicon carbide ceramics, Microchemical Journal 97 (2011) 101–108.